

# Flavor Diagonal and Off-Diagonal Susceptibilities in a Quasiparticle Model of the Quark-Gluon Plasma

M. Bluhm<sup>1</sup> and B. Kämpfer<sup>1,2</sup>

<sup>1</sup>*Forschungszentrum Dresden-Rossendorf,  
PF 510119, 01314 Dresden, Germany*

<sup>2</sup>*Institut für Theoretische Physik, TU Dresden, 01062 Dresden, Germany*

(Dated: July 8, 2008)

## Abstract

The Taylor coefficients of flavor diagonal and off-diagonal susceptibilities as well as baryon number, isovector and electric charge susceptibilities are considered within a phenomenological quasiparticle model of the quark-gluon plasma and successfully compared with available lattice QCD data up to fourth-order for two degenerate quark flavors. These susceptibility coefficients represent sensible probes of baryon density effects in the equation of state. The baryon charge is carried, in our model, by quark-quasiparticle excitations for hard momenta.

PACS numbers: 12.38.Mh;25.75-q;25.75.Ld

Keywords: quark-gluon plasma, susceptibility, quasiparticle model

## I. INTRODUCTION

The last few years witnessed two important milestones in the realm of relativistic heavy-ion collisions and related applied QCD: (i) Hints for a strongly coupled quark-gluon plasma have been deduced from experiments at RHIC [1–3], and (ii) lattice QCD calculations have been extended to non-zero net baryon density. While for many observables, at mid-rapidity, baryon-density effects are fairly small in heavy-ion collisions at top RHIC and future LHC energies, they become important for the ongoing low-energy runs at RHIC, previous CERN-SPS and future FAIR energies. Furthermore, the debated QCD critical point seems to be located at non-zero net baryon density according to investigations reported in [4]. Therefore, the exploration of this part of the phase diagram of strongly interacting matter gains increasing attention, both experimentally and theoretically. A necessary prerequisite in the search of the critical point is the understanding of thermodynamic bulk properties of QCD matter at non-zero net baryon density.

First-principle lattice QCD calculations include all features of the complexity of QCD at finite temperature and net baryon density, supposed the numerical accuracy is appropriate. Indeed, signals of the QCD critical point have been found [5, 6], and the pseudo-critical curve not too far from the temperature axis in the  $T - \mu$  plane is routinely determined today [5, 7] ( $T$  and  $\mu$  denote temperature and chemical potential, respectively).

Basically, the partition function  $Z(T, \mu)$  or the grand canonical potential  $\Omega(T, \mu)$  or the pressure  $p(T, \mu)$  contain much information on thermodynamic bulk properties of a medium. Susceptibilities are second-order derivatives of the pressure in the chemical potential direction. In so far, susceptibilities represent sensible quantities probing the active baryonic degrees of freedom in a medium. Even more, susceptibilities are related to fluctuations, which are debated to represent signatures of deconfinement effects [8, 9], thus being of utmost experimental relevance.

Information on various susceptibilities have been accumulated from first-principle lattice QCD calculations [6, 10–17]. Keeping in mind possible limitations due to finite-size, numerical set-up and quark mass ( $m_i$ ) effects they, nevertheless, are a source of important information on baryon density effects in the hot quark-gluon medium. Below  $T_c$ , where  $T_c$  denotes the pseudo-critical temperature for deconfinement, the hadron resonance gas model (cf. [12, 18]) has been successfully compared with the lattice QCD data [12]. Above  $T_c$ , the

situation is less settled. Certain baryonic bound states have been considered in [19] aiming at arriving at a physical picture of the strongly coupled quark-gluon plasma. Further developments [20, 21] try to deduce also transport properties of deconfined strongly interacting matter. In addition, susceptibilities have been studied in phenomenological approaches such as the Nambu–Jona-Lasinio model [22] or Polyakov loop extensions thereof [23–25] as well as quasiparticle models [26, 27]. Furthermore, within the  $\Phi$  functional approach to QCD [28], qualitative agreement with the lattice QCD data in [10] was found for  $T \geq 1.5 T_c$ . All these approaches attempt to catch the relevant excitation modes. One should keep in mind that in the weak-coupling regime or in a medium with prominent quasiparticle excitations, the bulk properties are governed by excitations with hard momenta  $k \sim T, \mu$ . Soft or ultra-hard modes are expected to influence  $p(T, \mu)$  rather less.

For the ultimate description of the very nature of the quark-gluon plasma one has to know correlations and spectral functions, propagators and related dispersion relations. Such information is still fairly scarce, but starts accumulating [29, 30]. Having at our disposal only the numerical data of thermodynamic state variables one must try to figure out which physical picture(s) is (are) compatible. Such an endeavor is clearly phenomenological. Besides the motivation of getting an interpretation of the available lattice QCD data, also the applicability of such phenomenological models represents important aspects, say for extrapolations to larger net baryon density, or for interpolations between different regions of the QCD equation of state (EoS) [27], or for comparing different flavor numbers.

The aim of the present paper is to confront in some detail the lattice QCD data from [6, 12, 13] for two degenerate quark flavors with our quasiparticle model [31–33]. This model was used up to now for one independent chemical potential. With the goal of analyzing isovector, electric charge and flavor (off-)diagonal susceptibilities we are going to generalize the model towards two independent chemical potentials  $\mu_u$  and  $\mu_d$  of up and down quarks, respectively. In fact, isovector and flavor (off-)diagonal susceptibilities represent much more sensible tests of a model than the baryon susceptibility alone. Furthermore, a detailed knowledge about the dependence of bulk thermodynamic quantities on, at least, two separate quark chemical potentials  $\mu_u$  and  $\mu_d$  is necessary in order to discuss the impact of changes in various flavor sectors on the baryon density dependence of the EoS. Also, this becomes important when discussing properties of deconfined quark matter such as  $\beta$ -stability and electric charge neutrality in hypothetical ultra-dense and hot proto-neutron stars. While for

one independent chemical potential, say  $\mu_u = \mu_d$ , the model has been successfully compared with various sets of lattice QCD data in [33, 34], the straightforward generalization to a set of chemical potentials  $\vec{\mu} = \{\mu_u, \mu_d\}$  is restricted by consistency requirements [35] given by Maxwell type relations and the stationarity condition of the thermodynamic potential. We show here, that the Taylor expansion coefficients of various susceptibilities are accessible up to a certain order in a consistent formulation, contrasting our model as an alternative to the picture developed, for instance, in [19].

Our paper is organized as follows. In section II, we extend the previous quasiparticle model [31–33] towards including two independent chemical potentials and discuss the consistency conditions for the resulting generalized system of flow equations. Section III is devoted to the numerical evaluation of various susceptibilities and the comparison with lattice QCD data. In addition, these results are used for discussing some properties of hot deconfined quark matter by means of a Taylor expansion of bulk thermodynamic quantities imposing, for instance,  $\beta$ -equilibrium and electric charge neutrality. The summary and discussion can be found in section IV. Appendix A summarizes the entropy density expression and its relation to the primary thermodynamic potential, while explicit representations of coefficients needed for determining the susceptibilities are listed in Appendices B, C and D.

## II. EXTENDING THE QUASIPARTICLE MODEL

We consider the case of two degenerate quark flavors for which the lattice QCD data [6, 12, 13] are at our disposal. We choose the pressure  $p(T, \mu_u, \mu_d) = \frac{T}{V} \ln Z(T, \mu_u, \mu_d)$  as fundamental quantity in the following with quark flavor chemical potentials  $\mu_{u,d}$  or, equivalently, quark and isovector chemical potentials  $\mu_{q,I}$  which are related via  $\mu_q = \frac{1}{2}(\mu_u + \mu_d)$ ,  $\mu_I = \frac{1}{2}(\mu_u - \mu_d)$  or  $\mu_u = \mu_q + \mu_I$ ,  $\mu_d = \mu_q - \mu_I$ . (Note that  $\mu_I$  was defined differently as either  $\mu_I = 2(\mu_u - \mu_d)$  in [11] or  $\mu_I = \frac{1}{4}(\mu_u - \mu_d)$  in [6, 13].)  $\mu_q = \frac{1}{3}\mu_B$  and  $\mu_I$  are associated with conserved quantum numbers (in strong interaction processes) of baryon number and isospin, respectively. The explicit model expression of  $p(T, \mu_u, \mu_d)$  is relegated to Appendix A. The generalized quark number susceptibilities are defined by

$$\chi_{j_u, j_d}(T) = \left. \frac{\partial^{(j_u + j_d)} p(T, \mu_u, \mu_d)}{\partial \mu_u^{j_u} \partial \mu_d^{j_d}} \right|_{\mu_u = \mu_d = 0}. \quad (1)$$

Because  $\ln Z(T, \mu_u, \mu_d)$  is symmetric under CP transformations, derivatives for odd  $(j_u + j_d)$  vanish. Furthermore, in the flavor symmetric case  $m_u = m_d = m$ , we find  $\chi_{j_u, j_d}(T) = \chi_{j_d, j_u}(T)$ .

These generalized quark number susceptibilities represent a rich test ground. Besides the mentioned physical meaning of susceptibilities as measures for fluctuations, they additionally constitute the Taylor coefficients of the excess pressure  $\Delta p(T, \mu_u, \mu_d) \equiv p(T, \mu_u, \mu_d) - p(T, \mu_u = 0, \mu_d = 0)$ , expanded simultaneously in powers of  $\mu_u$  and  $\mu_d$  via

$$\Delta p(T, \mu_u, \mu_d) = \sum_{j_u, j_d} \chi_{j_u, j_d}(T) \frac{\mu_u^{j_u}}{j_u!} \frac{\mu_d^{j_d}}{j_d!}, \quad (2)$$

thus containing information about baryon density effects in the EoS. (Similarly, one could consider the Taylor expansion of the pressure  $p(T, \mu_q + \mu_I, \mu_q - \mu_I)$  in terms of  $\mu_q$  and  $\mu_I$ .) Various associated expansion coefficients, e. g. those of flavor diagonal and off-diagonal susceptibilities as well as relations among them, are discussed below. The excess pressure becomes increasingly important in the domain of larger values of  $\mu_{u,d}$  and lower temperatures. For instance, imposing  $\beta$ -stability and electric charge neutrality of hot quark matter stars requires the knowledge about the dependence of bulk thermodynamic quantities on  $\mu_u$  and  $\mu_d$  separately, at least. This underscores the importance of the susceptibilities  $\chi_{j_u, j_d}(T)$  even if, at small  $T$ , a Taylor expansion in  $\mu_{u,d}$  directions may not suffice.

The net quark flavor number densities  $n_i = \partial p / \partial \mu_i$  with  $i = u, d$  read

$$n_i = \frac{d_i}{2\pi^2} \int_0^\infty dk k^2 \left[ \frac{1}{e^{(\omega_i - \mu_i)/T} + 1} - \frac{1}{e^{(\omega_i + \mu_i)/T} + 1} \right], \quad (3)$$

where  $d_i = d_{u,d} = 2 N_c$  refers to the spin and color degeneracies of the quarks. This implies that baryon charge- $\frac{1}{3}$  carriers are quasiparticles with quark quantum numbers obeying the dispersion relations [36]

$$\omega_i^2 = k^2 + m_i^2 + \Pi_i, \quad \Pi_i = \frac{1}{3} \left( T^2 + \frac{\mu_i^2}{\pi^2} \right) G^2(T, \mu_u, \mu_d). \quad (4)$$

For later purposes, we also exhibit the corresponding expression for gluons reading

$$\omega_g^2 = k^2 + \Pi_g, \quad \Pi_g = \frac{2}{3} \left( T^2 + \frac{3}{8\pi^2} (\mu_u^2 + \mu_d^2) \right) G^2(T, \mu_u, \mu_d). \quad (5)$$

The quark mass parameters  $m_i$  might comply with the lattice calculational set-up, e.g. either  $m_i = \xi_i T$  with constant  $\xi_i$  to compare with [12], or constant  $m_i$  to compare with [6, 13].

The crucial point is that, besides the displayed explicit dependence of the self-energy parts  $\Pi_l$  (where  $l$  is a label for  $u, d, g$ ) on  $\{\mu_i\} = \mu_{u,d}$  and  $T$ , there is also an implicit dependence via the effective coupling  $G^2(T, \mu_u, \mu_d)$ . In the case of one independent chemical potential  $\mu_u = \mu_d = \mu_q$  (i. e.  $\mu_I = 0$ ), the Maxwell relation  $\partial n_q / \partial T = \partial s / \partial \mu_q$ , with entropy density  $s$ , together with the stationarity of the grand canonical potential,  $\delta p / \delta \Pi_l = 0$ , leads to Peshier's flow equation [32] which determines  $G^2(T, \mu_q)$  for given initial condition  $G^2(T, \mu_q = 0)$ . In the case of two independent chemical potentials  $\mu_{u,d}$  or, equivalently,  $\mu_{q,I}$ , a system of three coupled equations is obtained from demanding stationarity and from the Maxwell relations

$$\frac{\partial s}{\partial \mu_I} = \frac{\partial n_I}{\partial T}, \quad (6)$$

$$\frac{\partial s}{\partial \mu_q} = \frac{\partial n_q}{\partial T}, \quad (7)$$

$$\frac{\partial n_I}{\partial \mu_q} = \frac{\partial n_q}{\partial \mu_I}. \quad (8)$$

The needed expression for the entropy density is listed in Appendix A and, with the definitions of  $\mu_{u,d}$  and  $\mu_{q,I}$  above, we note for isovector and quark number densities  $n_I = n_u - n_d$  and  $n_q = 3n_B = n_u + n_d$ , respectively. The emerging system generalizes Peshier's flow equation [32] towards two independent chemical potentials propagating  $G^2(T, \mu_q = 0, \mu_I = 0)$  into the thermodynamic parameter space, i. e. to non-zero  $\mu_q$  and  $\mu_I$ .

The structure of the generalized system of flow equations reads in the basis  $(\mu_q, \mu_I)$

$$A_1 \frac{\partial G^2}{\partial \mu_I} + B_1 \frac{\partial G^2}{\partial T} = C_1, \quad (9)$$

$$A_2 \frac{\partial G^2}{\partial \mu_q} + B_2 \frac{\partial G^2}{\partial T} = C_2, \quad (10)$$

$$(A_3 - B_3) \frac{\partial G^2}{\partial \mu_q} = (A_3 + B_3) \frac{\partial G^2}{\partial \mu_I}, \quad (11)$$

with coefficients  $A_{1,2,3}$ ,  $B_{1,2,3}$ ,  $C_{1,2}$  listed in Appendix B. From these coefficients it becomes evident how quark and gluon sectors are coupled. It was earlier argued [35] that the generalized system of flow equations in Eqs. (9-11) cannot be solved uniquely for arbitrary values of  $\mu_q$  and  $\mu_I$ , but only when assuming a side condition  $\mu_u = \mu_u(\mu_d)$ , i. e. when considering merely one independent chemical potential. To see this, we reformulate Eqs. (9-11) in the basis  $(\mu_u, \mu_d)$ , making use of the analog of Eq. (11) in terms of  $\mu_u$  and  $\mu_d$ . Then, the

generalized system of flow equations is transformed into

$$\mathcal{A}_1 \frac{\partial G^2}{\partial \mu_u} + \mathcal{B}_1 \frac{\partial G^2}{\partial T} = \mathcal{C}_1, \quad (12)$$

$$\mathcal{A}_2 \frac{\partial G^2}{\partial \mu_u} + \mathcal{B}_2 \frac{\partial G^2}{\partial T} = \mathcal{C}_2. \quad (13)$$

These partial differential equations are uniquely solvable if the coefficients  $\mathcal{A}_{1,2}$  and  $\mathcal{B}_{1,2}$  and  $\mathcal{C}_{1,2}$ , as listed in Appendix C, are pairwise equal. Indeed,  $\mathcal{A}_1 = \mathcal{A}_2$  and  $\mathcal{B}_1 = \mathcal{B}_2$  hold in general. But, the furthermore needed equality  $\mathcal{C}_1 = \mathcal{C}_2$  is ensured for arbitrary but small values of  $\mu_{u,d}$ , i. e.  $\mu_{u,d} \ll \pi T$ . (Actually, the equality of  $\mathcal{C}_1$  and  $\mathcal{C}_2$  is given up to order  $\mathcal{O}(\mu_{u,d}^2)$  in a Taylor series expansion in terms of  $\mu_u$  and  $\mu_d$ ; the coefficients of third-order terms start to differ.)

As the primary goal of this paper is the comparison of susceptibility Taylor series expansion coefficients Eq. (1) (to be calculated as derivatives of  $p$  at  $\mu_{u,d} = 0$ ) with lattice QCD results up to fourth-order, the necessary conditions are fulfilled. The issue of potential limitations provided by the restriction to the small  $\mu_{u,d}$  region and one possible way of circumventing them are discussed in Appendix D. In the needed leading order for evaluating the susceptibility coefficients of interest we note that from Eqs. (56) and (57) in Appendix C

$$\mu_u = \mu_d \frac{\mathcal{I}_1}{\mathcal{I}_2}, \quad (14)$$

$$\mu_u = \mu_d \frac{\mathcal{I}_5}{\mathcal{I}_4} \frac{\mathcal{I}_1}{\mathcal{I}_2}, \quad (15)$$

where  $\mathcal{I}_k$  represent phase-space integrals listed in Appendix B, implying also  $\omega_u = \omega_d$  in the mass symmetric case,  $m_u = m_d$ , and  $\mathcal{I}_4 = \mathcal{I}_5$ .

Furthermore, by exploiting Eqs. (9-11), one finds  $\left. \frac{\partial G^2}{\partial \mu_q} \right|_{\mu_q=\mu_I=0} = \left. \frac{\partial G^2}{\partial \mu_I} \right|_{\mu_q=\mu_I=0} = 0$  and

$$\begin{aligned} \left. \frac{\partial^2 G^2}{\partial \mu_q^2} \right|_{\mu_q=\mu_I=0} &= \frac{1}{\mathcal{N}} \left\{ \mathcal{N}_1 \left[ 2\xi_u^2 T + \frac{2}{3} T G^2(T) + \frac{1}{3} T^2 \frac{\partial G^2(T)}{\partial T} \right] \right. \\ &\quad + \mathcal{N}_2 \left[ 2\xi_d^2 T + \frac{2}{3} T G^2(T) + \frac{1}{3} T^2 \frac{\partial G^2(T)}{\partial T} \right] \\ &\quad \left. - \mathcal{I}_3 \frac{1}{\pi^2} G^2(T) - \mathcal{I}_4 \frac{2}{3\pi^2} G^2(T) - \mathcal{I}_5 \frac{2}{3\pi^2} G^2(T) \right\}, \end{aligned} \quad (16)$$

while from Eqs. (12) and (13), we find  $\left. \frac{\partial G^2}{\partial \mu_u} \right|_{\mu_u=\mu_d=0} = \left. \frac{\partial G^2}{\partial \mu_d} \right|_{\mu_u=\mu_d=0} = 0$  and

$$\begin{aligned} \left. \frac{\partial^2 G^2}{\partial \mu_u^2} \right|_{\mu_u=\mu_d=0} &= \frac{1}{\mathcal{N}} \left\{ \mathcal{N}_1 \left[ 2\xi_u^2 T + \frac{2}{3} T G^2(T) + \frac{1}{3} T^2 \frac{\partial G^2(T)}{\partial T} \right] \right. \\ &\quad \left. - \mathcal{I}_3 \frac{1}{2\pi^2} G^2(T) - \mathcal{I}_4 \frac{2}{3\pi^2} G^2(T) \right\}, \end{aligned} \quad (17)$$

with coefficients  $\mathcal{N}$ ,  $\mathcal{N}_{1,2}$  listed in Appendix C,  $G^2(T) = G^2(T, \mu_u = 0, \mu_d = 0)$  and  $\mathcal{I}_{3,4,5}$  considered at  $\mu_q = \mu_I = 0$  or, equivalently,  $\mu_u = \mu_d = 0$ . Note that in the flavor symmetric case considered here, Eqs. (16) and (17) are related via  $\partial^2 G^2 / \partial \mu_u^2|_{\mu_{u,d}=0} = \frac{1}{2} \partial^2 G^2 / \partial \mu_q^2|_{\mu_{q,I}=0}$ . In addition, odd derivatives with respect to the chemical potentials such as  $\frac{\partial^3 G^2}{\partial \mu_u^3}$  or mixed derivatives such as  $\frac{\partial^2 G^2}{\partial \mu_u \partial \mu_d}$  or  $\frac{\partial^2 G^2}{\partial \mu_q \partial \mu_I}$  vanish at  $\mu_u = \mu_d = 0 = \mu_q = \mu_I$ . The above stated expressions and equalities are uniquely obtained from the generalized system of flow equations in the region of small  $\mu_{u,d}$ , and we can proceed by evaluating various susceptibilities.

### III. COMPARISON WITH LATTICE QCD DATA

#### A. Taylor expansions in $\mu_q/T$ at $\mu_I = 0$

In this section, we confront the above extended quasiparticle model (QPM) with lattice QCD data of various susceptibilities for  $N_f = 2$  degenerate quark flavors. In [12], quark number and isovector susceptibilities as well as flavor diagonal and off-diagonal susceptibilities have been calculated on a lattice with temporal and spatial extensions  $N_\tau = 4$  and  $N_\sigma = 16$  using improved actions and  $m_u = m_d = 0.4 T$  (i. e.  $\xi_u = \xi_d = 0.4$ ) as quark mass parameters. As a special case of the Taylor expansion in terms of  $\mu_q$  and  $\mu_I$ , expansions in terms of  $\mu_q/T$  at  $\mu_I = 0$  were considered.

The quark number susceptibility  $\chi_q(T, \mu_q)/T^2 = \frac{\partial^2(p(T, \mu_q, \mu_q)/T^4)}{\partial(\mu_q/T)^2} = 2c_2 + 12c_4 \left(\frac{\mu_q}{T}\right)^2 + 30c_6 \left(\frac{\mu_q}{T}\right)^4 + \mathcal{O}(\mu_q^6)$  with  $c_k(T) = \frac{1}{k!} \frac{\partial^k(T^{-4}p(T, \mu_q + \mu_I, \mu_q - \mu_I))}{\partial(\mu_q/T)^k} \Big|_{\mu_{q,I}=0}$  has been analyzed already in detail in [33], and an impressively good agreement of our model with the lattice QCD data from [12] has been found. The isovector susceptibility  $\chi_I(T, \mu_q)$  is only accessible with the present extension of our model; it obeys the expansion

$$\frac{\chi_I(T, \mu_q)}{T^2} = \frac{\partial^2(p(T, \mu_q + \mu_I, \mu_q - \mu_I)/T^4)}{\partial(\mu_I/T)^2} = 2c_2^I + 12c_4^I \left(\frac{\mu_q}{T}\right)^2 + 30c_6^I \left(\frac{\mu_q}{T}\right)^4 + \mathcal{O}(\mu_q^6), \quad (18)$$

where the expansion coefficients read

$$c_k^I(T) = \frac{1}{k!} \frac{\partial^k(T^{-4}p(T, \mu_q + \mu_I, \mu_q - \mu_I))}{\partial(\mu_I/T)^2 \partial(\mu_q/T)^{k-2}} \Big|_{\mu_{q,I}=0}. \quad (19)$$

Due to the invariance of  $\ln Z$  under CP transformations,  $c_k^I$  vanish for odd  $k$ .

For the first coefficient of interest we find within the extended QPM the explicit repre-



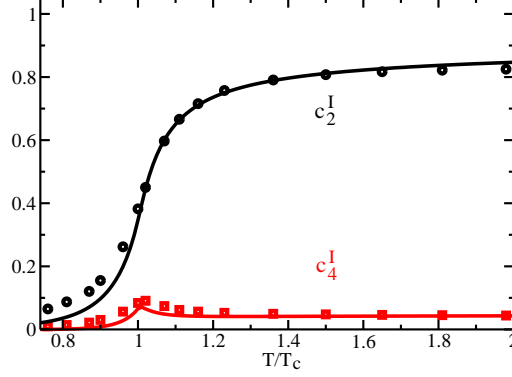


FIG. 1: (color online). Comparison of QPM results (solid curves) for  $c_k^I$  with lattice QCD data [12] (circles for  $k = 2$  and squares for  $k = 4$ ) for  $N_f = 2$  quark flavors.

sentation

$$c_2^I(T) = \frac{d}{\pi^2} \int_0^\infty dk \frac{k^2}{T^3} \frac{e^{\epsilon_0}}{(e^{\epsilon_0} + 1)^2}, \quad (20)$$

with  $d = d_u = d_d$  and  $\epsilon_0 = \omega_u/T|_{\mu_u, d=0} = \omega_d/T|_{\mu_u, d=0}$  which implies  $c_2^I = c_2$  for all temperatures (cf. [33]) in the QPM. The next non-zero coefficient is

$$c_4^I(T) = \frac{d}{12\pi^2} \int_0^\infty dk \frac{k^2}{T^3} \frac{e^{\epsilon_0}}{(e^{\epsilon_0} + 1)^4} \left\{ e^{2\epsilon_0} - 4e^{\epsilon_0} + 1 - \frac{(e^{2\epsilon_0} - 1)}{\epsilon_0} \left( \frac{1}{\pi^2} G^2(T) + \frac{T^2}{6} \frac{\partial^2 G^2}{\partial \mu_q^2} \Big|_{\mu_q, I=0} \right) \right\}, \quad (21)$$

where  $\frac{\partial^2 G^2}{\partial \mu_q^2} \Big|_{\mu_q, I=0}$  is given in Eq. (16).

As in our previous studies [33], we choose for the effective coupling  $G^2(T, \mu_u = 0, \mu_d = 0)$  entering Eqs. (4), (5) and (16) the parametrization

$$G^2(T) = \begin{cases} G_{2\text{loop}}^2(\zeta), & \zeta = \lambda \frac{(T-T_s)}{T_c}, \quad T \geq T_c, \\ G_{2\text{loop}}^2(T_c) + b(1 - \frac{T}{T_c}), & T < T_c. \end{cases} \quad (22)$$

The numerically evaluated QPM results for  $c_2^I$  and  $c_4^I$  are exhibited in Fig. 1 (results for  $c_{2,4}$  are exhibited in [33]) and compared with lattice QCD data [12], where we use as parameters entering  $G^2(T)$  in Eq. (22)  $\lambda = 5.95$ ,  $T_s = 0.75 T_c$  and  $b = 421.5$ . The explicit value of  $T_c$  is not important for the scaled quantities considered here. (Note that these parameters differ from the parametrization employed in [33] for describing  $c_i$ . This is due to the different quark dispersion relations used in [33] and here. Employing instead Eq. (4) as quark dis-

persion relation with the QPM parameters for  $G^2(T)$  stated above, we find an equally good agreement of QPM results for  $c_i$  with the lattice QCD data [12] as reported in [33].)

Similar to  $c_4$ , the expansion coefficient  $c_4^I$  slightly underestimates the lattice QCD data [12] approaching its Stefan-Boltzmann limit  $1/(2\pi^2)$ , while  $c_2^I$  agrees remarkably well with the data [12] for  $T \geq T_c$  approaching its Stefan-Boltzmann limit  $N_f/2$  asymptotically. Whereas  $\chi_q$ , due to the growing importance of the higher-order expansion coefficients with increasing chemical potential, exhibits a significant peak structure close to  $T_c$  for large  $\mu_q/T$  indicating some critical behavior,  $\chi_I$  does not point to such structures. This behavior is a consequence of the much less pronounced peak in  $c_4^I$  compared to  $c_4$ . Similar findings were reported in [37], where a phenomenological sigma model was considered. Below  $T_c$ , the agreement with lattice QCD data might be accidental, but one may consider Eq. (22) as convenient parametrization also for this region (see also discussion in section IV).

Correlations between fluctuations in different flavor components can be discussed by considering flavor diagonal and off-diagonal susceptibilities. They read

$$\frac{\chi_{uu}}{T^2} = \frac{1}{4} \left( \frac{\chi_q}{T^2} + \frac{\chi_I}{T^2} \right) = 2c_2^{uu} + 12c_4^{uu} \left( \frac{\mu_q}{T} \right)^2 + 30c_6^{uu} \left( \frac{\mu_q}{T} \right)^4 + \mathcal{O}(\mu_q^6) \quad (23)$$

for the flavor diagonal susceptibility and

$$\frac{\chi_{ud}}{T^2} = \frac{1}{4} \left( \frac{\chi_q}{T^2} - \frac{\chi_I}{T^2} \right) = 2c_2^{ud} + 12c_4^{ud} \left( \frac{\mu_q}{T} \right)^2 + 30c_6^{ud} \left( \frac{\mu_q}{T} \right)^4 + \mathcal{O}(\mu_q^6) \quad (24)$$

for the flavor off-diagonal susceptibility, where the individual expansion coefficients are defined by  $c_k^{uu} = (c_k + c_k^I)/4$  and  $c_k^{ud} = (c_k - c_k^I)/4$ .

The expansion coefficients  $c_k^{uu}$  and  $c_k^{ud}$  for  $k = 2, 4$  are exhibited in Fig. 2 and compared with lattice QCD data [12]. The diagonal expansion coefficients  $c_{2,4}^{uu}$  show a similar pattern as  $c_{2,4}$  and  $c_{2,4}^I$  approaching their Stefan-Boltzmann limits  $N_f/4$  asymptotically in the case of  $c_2^{uu}$  and  $1/(4\pi^2)$  for  $T > 2T_c$  in the case of  $c_4^{uu}$ . The pronounced peak structure of the off-diagonal expansion coefficient  $c_4^{ud}$  is well reproduced, while in our extended QPM  $c_2^{ud}$  is zero for all temperatures, in contrast to the data which are numerically small and differ noticeably from zero only in the region  $T \lesssim T_c$ . This is simply a consequence of  $c_2^I = c_2$ . The pattern observed for the flavor off-diagonal susceptibility coefficients is discussed further in section III B. As the flavor off-diagonal susceptibility coefficients  $c_k^{ud}$  rapidly approach their Stefan-Boltzmann limit which is zero for all  $k$ ,  $\chi_{ud}$  vanishes for large  $T$  indicating that fluctuations in different flavor channels are uncorrelated at high temperatures. On the other

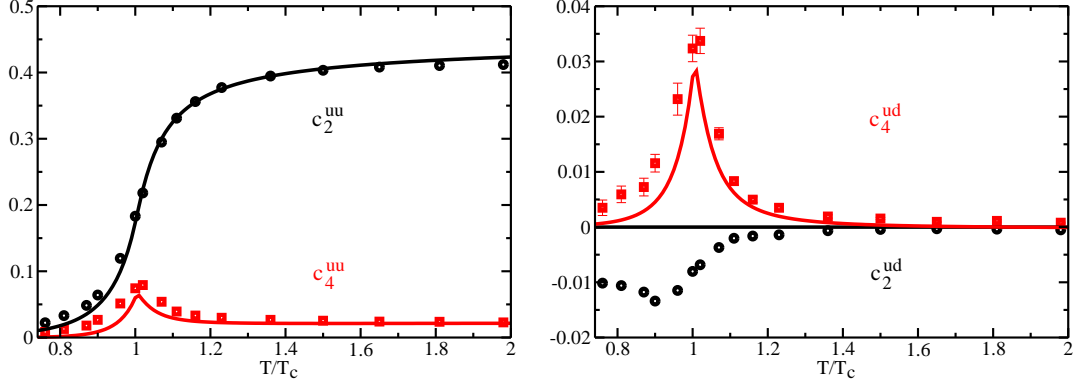


FIG. 2: (color online). Comparison of QPM results (solid curves) for the expansion coefficients  $c_k^{uu}$  of the flavor diagonal susceptibility  $\chi_{uu}$  (left) and  $c_k^{ud}$  of the flavor off-diagonal susceptibility  $\chi_{ud}$  (right) with lattice QCD data [12] (circles for  $k = 2$ , squares for  $k = 4$ ).

hand,  $\chi_{ud}$  increases rapidly with increasing  $\mu_q$  in the vicinity of  $T_c$ , indicating increasing correlations [8, 9] between fluctuations in different flavor channels in the transition region. This also explains the observed different behavior of  $\chi_q$  and  $\chi_I$ : While peak structures effectively add up in  $\chi_q$  they approximately cancel each other in  $\chi_I$ .

The behavior of the electric charge susceptibility  $\chi_Q$  is strongly related to  $\chi_q$  and  $\chi_I$  via  $\chi_Q = \frac{1}{4} (\chi_I + \frac{1}{9}\chi_q)$ . The corresponding Taylor expansion reads

$$\frac{\chi_Q(T, \mu_q)}{T^2} = 2c_2^Q + 12c_4^Q \left(\frac{\mu_q}{T}\right)^2 + 30c_6^Q \left(\frac{\mu_q}{T}\right)^4 + \mathcal{O}(\mu_q^6), \quad (25)$$

with expansion coefficients  $c_k^Q = \frac{1}{4} (c_k^I + \frac{1}{9}c_k^q) = (\frac{5}{9}c_k^{uu} - \frac{4}{9}c_k^{ud})$ . The coefficients  $c_2^Q$  and  $c_4^Q$  are exhibited in Fig. 3. From the definition of  $c_k^Q$  it becomes clear that contributions of pronounced structures appearing in flavor diagonal and off-diagonal susceptibilities do not completely cancel in the electric charge susceptibility.

## B. Taylor expansion in $\mu_u$ and $\mu_d$

In this section, we confront the extended QPM with lattice QCD data [6, 13] of generalized quark number susceptibilities  $\chi_{j_u, j_d}$  as defined in Eq. (1). These simulations were also performed for  $N_f = 2$  degenerate quark flavors on a lattice with temporal and spatial extensions  $N_\tau = 4$  and  $N_\sigma = 16$ . However, the used quark mass parameter entering the quark dispersion relation reads now  $m_u = m_d = 0.1 T_c$ , in agreement with the lattice performance [6, 13], which is temperature independent in contrast to the lattice set-up considered

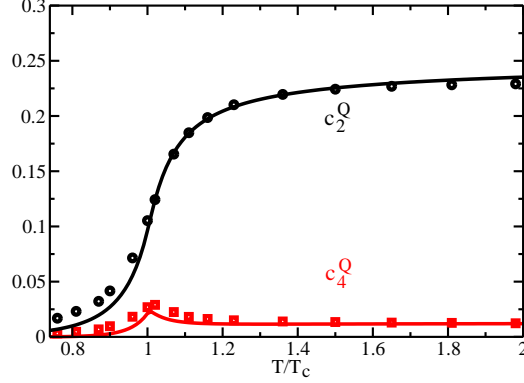


FIG. 3: (color online). Comparison of QPM results (solid curves) for the electric charge susceptibility coefficients  $c_k^Q$  with lattice QCD data [12] (circles for  $k = 2$ , squares for  $k = 4$ ).

in section III A. As a result, some of the coefficients in the generalized system of flow equations render which changes also the derivative expressions of the effective coupling. To be precise, the terms explicitly depending on  $\xi_u$  and  $\xi_d$ , which enter Eqs. (16) and (17) and some coefficients in Appendix B and C, have to vanish for constant  $m_{u,d}$ .

Furthermore, non-improved actions have been employed in [6, 13], thus cut-off effects on the numerical results are sizeably increased compared to improved actions. In section III A, we assumed the lattice QCD data [12] to be rather close to the continuum limit as improved actions were used (cf. a discussion in [38]); thus no continuum correction factor was applied. (As discussed in [11], continuum limit corrections to the Taylor expansion coefficients  $c_k$  are expected to be similar (10-20%) to corrections for the pressure at zero chemical potential [39], even though, the corrections seem to increase for higher-order expansion coefficients, see [11, 40].) Here, however, we have to rely on an estimate for the continuum extrapolation of the lattice QCD data from [6, 13]. By investigating different temporal lattice extensions  $N_\tau$  at fixed large temperature in [41, 42], the continuum limit of some generalized quark number susceptibilities was estimated. Even though, in principle, correction factors could be different for different temperatures, we apply as scaling factors  $d_{lat}^{(\chi_2)} = 0.47$  in the case of  $\chi_{2,0}/T^2$  [41, 42] and a larger correction  $d_{lat}^{(\chi_4)} = 0.32$  in the case of  $\chi_{4,0}$  [42] to the data [6, 13] for all  $T$ .

Estimating the continuum limit is necessary for making possible a meaningful comparison between the expansion coefficients considered in section III A and the generalized quark number susceptibilities  $\chi_{j_u, j_d}$ . In fact, they are closely related [19], e. g. the expansion

coefficients of flavor diagonal and off-diagonal susceptibilities  $\chi_{uu}$  and  $\chi_{ud}$  can be expressed in terms of  $\chi_{j_u, j_d}$  via

$$c_2^{uu} = \frac{1}{2} \frac{\chi_{2,0}}{T^2}, \quad (26)$$

$$c_2^{ud} = \frac{1}{2} \frac{\chi_{1,1}}{T^2}, \quad (27)$$

$$c_4^{uu} = \frac{1}{24} (\chi_{4,0} + 2\chi_{3,1} + \chi_{2,2}), \quad (28)$$

$$c_4^{ud} = \frac{1}{24} (2\chi_{3,1} + 2\chi_{2,2}). \quad (29)$$

Within the extended QPM, we find from Eq. (1) and by using Eqs. (28) and (29)

$$\frac{\chi_{2,0}(T)}{T^2} = \frac{d}{\pi^2} \int_0^\infty dk \frac{k^2}{T^3} \frac{e^{\epsilon_0}}{(e^{\epsilon_0} + 1)^2}, \quad (30)$$

$$\chi_{1,1}(T) = 0, \quad (31)$$

$$\chi_{4,0}(T) = \frac{d}{\pi^2} \int_0^\infty dk \frac{k^2}{T^3} \frac{e^{\epsilon_0}}{(e^{\epsilon_0} + 1)^4} \left\{ e^{2\epsilon_0} - 4e^{\epsilon_0} + 1 - \frac{(e^{2\epsilon_0} - 1)}{\epsilon_0} \left( \frac{1}{\pi^2} G^2(T) + \frac{T^2}{2} \frac{\partial^2 G^2}{\partial \mu_u^2} \Big|_{\mu_{u,d}=0} \right) \right\}, \quad (32)$$

$$\chi_{3,1}(T) = -\frac{d}{\pi^2} \int_0^\infty dk \frac{k^2}{T^3} \frac{e^{\epsilon_0}}{(e^{\epsilon_0} + 1)^4} \frac{(e^{2\epsilon_0} - 1)}{\epsilon_0} \frac{T^2}{2} \left( \frac{1}{2} \frac{\partial^2 G^2}{\partial \mu_q^2} \Big|_{\mu_{q,I}=0} - \frac{\partial^2 G^2}{\partial \mu_u^2} \Big|_{\mu_{u,d}=0} \right), \quad (33)$$

$$\chi_{2,2}(T) = -\frac{d}{\pi^2} \int_0^\infty dk \frac{k^2}{T^3} \frac{e^{\epsilon_0}}{(e^{\epsilon_0} + 1)^4} \frac{(e^{2\epsilon_0} - 1)}{\epsilon_0} \frac{T^2}{2} \left( \frac{\partial^2 G^2}{\partial \mu_u^2} \Big|_{\mu_{u,d}=0} - \frac{1}{3} \frac{\partial^2 G^2}{\partial \mu_q^2} \Big|_{\mu_{q,I}=0} \right), \quad (34)$$

where  $\frac{\partial^2 G^2}{\partial \mu_q^2} \Big|_{\mu_{q,I}=0}$  and  $\frac{\partial^2 G^2}{\partial \mu_u^2} \Big|_{\mu_{u,d}=0}$  are given in Eqs. (16) and (17). As both derivatives of the effective coupling entering these expressions are related with each other in the flavor symmetric case, we find  $\chi_{3,1} = 0$  for all temperatures in the QPM, while  $\chi_{2,2}$  is non-zero. Furthermore,  $\chi_{1,1} = 0$  as  $c_2^{ud}$  vanishes for all temperatures, while  $c_4^{ud}$  is non-zero as  $\chi_{2,2}$  is non-zero. In particular  $\chi_{1,1}$ , or  $c_2^{ud}$ , vanishes because flavor-mixing effects, which describe the dependence of one quark flavor sector on changes in another one, are inherent in the quasiparticle model only via the quasiparticle dispersion relations resulting in terms which vanish at  $\mu_{u,d} = 0$ . Qualitatively, our findings, in particular the observed deviations in the flavor off-diagonal susceptibility coefficients, can be understood from perturbative QCD arguments. In a perturbative expansion of the thermodynamic potential different partonic sectors start to couple only at order  $\mathcal{O}(g^3)$  of the QCD running coupling  $g$ . However, these plasmon term contributions  $\propto g^3$  are not completely reproduced in a similar expansion of the quasiparticle model thermodynamic potential [43]. Similar findings, pointing to the necessity

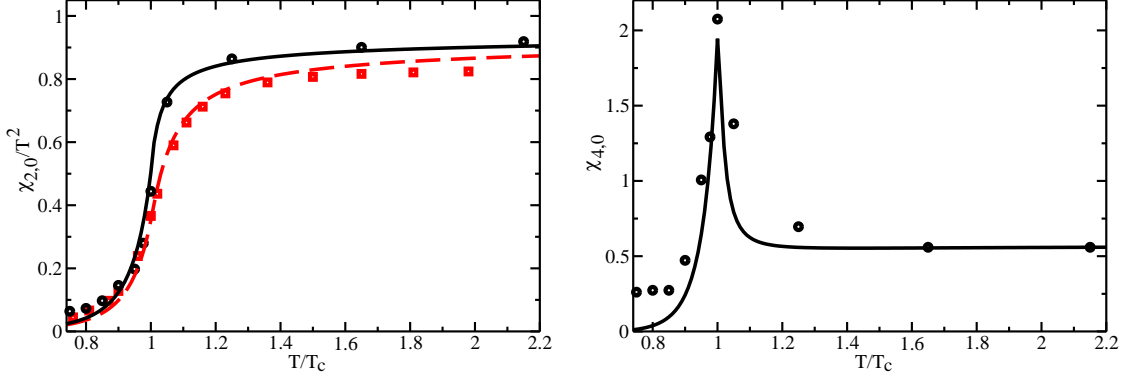


FIG. 4: (color online). Comparison of QPM results (dashed curves for the parametrization employed in section III A and solid curves for readjusted QPM parameters) for the generalized quark number susceptibilities  $\chi_{2,0}/T^2$  (left panel) and  $\chi_{4,0}$  (right panel) with the continuum extrapolated lattice QCD data [6, 13] (circles) and the lattice QCD data for  $2c_2^{uu}$  from [12] (squares).

of properly including flavor-mixing effects for affecting the flavor off-diagonal susceptibility, were reported in [44] within a Polyakov loop extended Nambu–Jona-Lasinio model approach.

In Fig. 4, we exhibit the QPM results for  $\chi_{2,0}/T^2$  and  $\chi_{4,0}$  and compare with the continuum extrapolated lattice QCD data from [6, 13] (circles). When using the QPM parameters found in section III A, the QPM results (dashed curve in the left panel of Fig. 4) underestimate the lattice QCD data (circles) of  $\chi_{2,0}/T^2$ . For comparison, we also show the lattice QCD data [12] for  $2c_2^{uu}$  (squares), where the increasing deviations of the QPM results (dashed curve) from the data (squares) for increasing temperatures are due to the different quark mass parameters used here and in section III A. (Note that when applying continuum limit corrections of about 10% in the considered temperature range to the lattice QCD data [12] (squares) as stated above, both continuum extrapolated lattice QCD data sets [6, 13] (circles) and [12] would be fairly well compatible apart from a narrow interval around  $T \approx T_c$  such that one unique QPM parametrization would be sufficient.) To bridge the data for  $\chi_{2,0}$  to  $\chi_{4,0}$  by our model, we readjust, therefore, the QPM parameters entering  $G^2(T)$  in Eq. (22) in order to perfectly describe the lattice QCD data [6, 13] (circles) of  $\chi_{2,0}/T^2$  by using  $\lambda = 17$ ,  $T_s = 0.905 T_c$  and  $b = 431$ . The corresponding QPM results for  $\chi_{2,0}/T^2$  and  $\chi_{4,0}$  are exhibited by solid curves in Fig. 4. Again, very good agreement for  $T > 0.9 T_c$  is found.

### C. Deconfined $\beta$ -stable and electrically neutral quark matter

Now, we turn our attention to the discussion of some bulk properties of deconfined quark matter of  $N_f = 2$  dynamical quark flavors by means of Taylor series expansions using the generalized quark number susceptibilities discussed in the previous section. Clearly, these considerations are limited by the range of validity of such an approach, say by conservatively guessing the quark flavor chemical potentials to be individually restricted by  $\mu_{u,d}/T < 1$ . Note that we employ again  $m_{u,d} = 0.1 T_c$  as quark mass parameter.

Starting from the definition of the excess pressure  $\Delta p$  in Eq. (2), including only terms up to  $j_u + j_d = 4$ , the net baryon density  $n_B$ , suppressing the explicit notation of the temperature dependence inherent in the generalized quark number susceptibilities, reads

$$n_B(\mu_u, \mu_d) = \frac{1}{3} \left\{ (\chi_{2,0} + \chi_{1,1})(\mu_u + \mu_d) + \left( \frac{\chi_{4,0}}{3!} + \frac{\chi_{3,1}}{3!} \right) (\mu_u^3 + \mu_d^3) + \frac{1}{2} (\chi_{3,1} + \chi_{2,2})(\mu_u^2 \mu_d + \mu_u \mu_d^2) \right\}, \quad (35)$$

$$n_B(\mu_B, \mu_I) = \frac{1}{9} \left\{ 2(\chi_{2,0} + \chi_{1,1})\mu_B + \frac{1}{9} \left( \frac{1}{3}\chi_{4,0} + \frac{4}{3}\chi_{3,1} + \chi_{2,2} \right) \mu_B^3 + (\chi_{4,0} - \chi_{2,2})\mu_B \mu_I^2 \right\}. \quad (36)$$

Thus, the net baryon density simultaneously depends on two independent chemical potentials,  $\mu_u$  and  $\mu_d$  (or, equivalently,  $\mu_B$  and  $\mu_I$ ). This is similarly the case for a non-interacting gas of gluons and massless quarks with two independent quark flavor chemical potentials. Only in the special case of  $\mu_I = 0$ , i. e.  $\mu_u = \mu_d = \mu_q$ ,  $n_B$  is a function of one chemical potential  $\mu_B$  alone ensuring constant net baryon density for constant baryo-chemical potential. In general, however, a detailed knowledge about the dependence on different quark chemical potentials is required, when discussing baryon density effects on the EoS. This is illustrated in Fig. 5, where the scaled net baryon density is exhibited for constant  $\mu_B$  and constant temperatures. As by definition  $\mu_d = \frac{2}{3}\mu_B - \mu_u$ , one chemical potential in Eq. (35) can be replaced. We chose  $\mu_B/T = 1$  such that  $\mu_u/T + \mu_d/T = \frac{2}{3}$ , ensuring that these considerations stay within the range of validity of the employed Taylor expansion approach. The minimum at  $\mu_u/T = \mu_d/T = \frac{1}{3}$  exhibits the value of  $n_B/T^3$  for one independent quark chemical potential.  $n_B$  for  $\mu_B = T$  drops by 3.3% at  $T = 2T_c$  and by 4.6% at  $T = 1.05T_c$  when changing  $\mu_u/T$  from 0 to  $\frac{1}{3}$ . Accordingly, one is tempted to consider the detailed knowledge about the individual  $\mu_u$  and  $\mu_d$  dependencies as not so important.

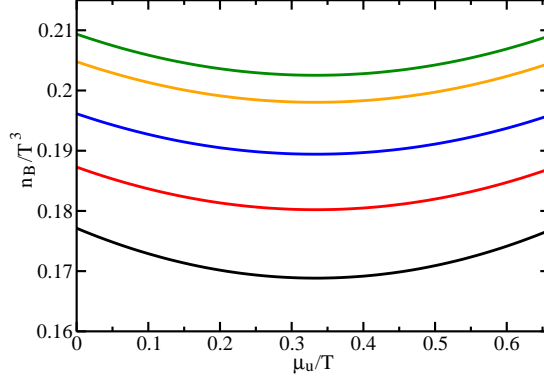


FIG. 5: (color online). Scaled net baryon density  $n_B/T^3$  from Eq. (35) for constant  $\mu_B/T = 1$  as a function of  $\mu_u/T$  for constant temperatures  $T/T_c = 2, 1.5, 1.2, 1.1, 1.05$  from top to bottom.

However, there are physical situations, where the corresponding side conditions require the separate knowledge about the non-trivial  $\mu_u$  and  $\mu_d$  dependencies of bulk thermodynamic quantities. First, we consider curves of constant  $\mu_B$ , which are given by the linear relation  $\mu_d = \frac{2}{3}\mu_B - \mu_u$  (see short-dashed curve in the left panel of Fig. 6 with  $\mu_B/T = 1$ ). The individual net quark number densities read  $n_u = \chi_{2,0}\mu_u + \chi_{1,1}\mu_d + \frac{\chi_{4,0}}{3!}\mu_u^3 + \frac{\chi_{3,1}}{2}\mu_u^2\mu_d + \frac{\chi_{3,1}}{3!}\mu_d^3 + \frac{\chi_{2,2}}{2}\mu_u\mu_d^2$  and  $n_d = \chi_{2,0}\mu_d + \chi_{1,1}\mu_u + \frac{\chi_{4,0}}{3!}\mu_d^3 + \frac{\chi_{3,1}}{2}\mu_u\mu_d^2 + \frac{\chi_{3,1}}{3!}\mu_u^3 + \frac{\chi_{2,2}}{2}\mu_u^2\mu_d$ . Since in the QPM  $\chi_{1,1} = \chi_{3,1} = 0$ , lines of constant  $n_u$  or  $n_d$  are approximately given by lines of constant  $\mu_u$  or  $\mu_d$ , i. e. simply vertical or horizontal lines in the left panel of Fig. 6 (not displayed). (Only at temperatures  $T \approx T_c$ , where  $\chi_{2,2}$  is non-negligible, the simple pattern is deformed somewhat.) This situation is completely different when considering constant scaled net baryon densities as depicted by the solid curve in Fig. 6 (left panel) for  $n_B/T^3 = 0.187$  at  $T = 1.1 T_c$  unravelling the non-trivial dependence of  $\mu_d$  on  $\mu_u$  in contrast to constant  $\mu_B$ . In fact, here  $\mu_B/T > 1$  except for the case when  $\mu_u/T = 0$  or  $\mu_d/T = 0$ .

In heavy-ion collisions one often relates the quantum numbers of the entrance channel with the ones of the emerging fireball. Isospin-symmetric nuclear matter, for instance, is characterized by an electric charge per baryon ratio of 1:2. This translates into  $\frac{2}{3}n_u - \frac{1}{3}n_d = \frac{1}{2}n_B$  which is fulfilled for  $\mu_d = \mu_u$ , i. e. simply a diagonal line in the left panel of Fig. 6 (not displayed). Discussing, instead, gold on gold collisions, the electric charge per baryon ratio is approximately 0.4. The corresponding dependence  $\mu_d(\mu_u)$  for  $T = 1.1 T_c$  is depicted by the dotted curve in the left panel of Fig. 6. Another important issue concerns electric charge neutrality in bulk matter. In pure  $N_f = 2$  quark matter, electric charge neutrality would



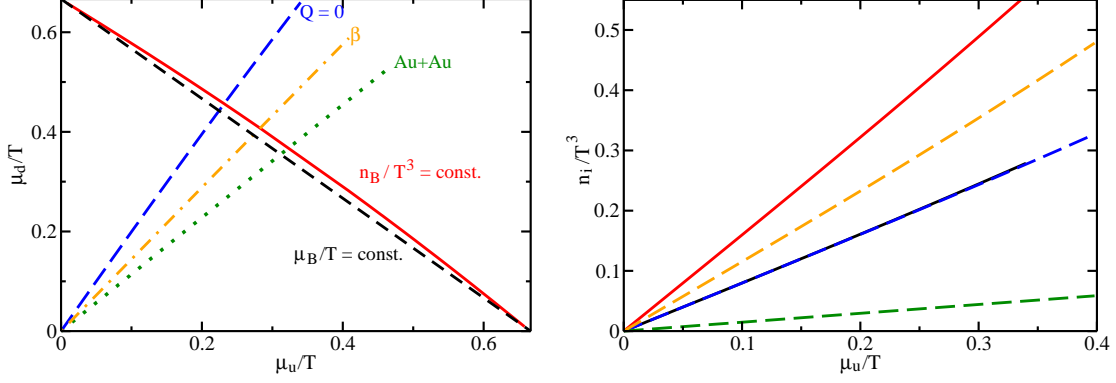


FIG. 6: (color online). Left: Dependence  $\mu_d(\mu_u)$  for various side conditions or physical situations.  $\mu_B = T$  is depicted by the short-dashed curve, whereas constant  $n_B/T^3 = 0.187$  holds along the solid curve where  $\mu_B \geq T$ . Electric charge neutrality is given along the long-dashed curve for pure  $N_f = 2$  quark matter, while the dash-dotted curve includes additionally electrons, imposing  $\beta$ -equilibrium. The dotted curve reflects the situation in  $Au + Au$  heavy-ion collisions. (The curves end where  $\mu_u/T + \mu_d/T \geq 1$ .) Right: Scaled net number densities as functions of  $\mu_u/T$  demanding electric charge neutrality either for pure  $N_f = 2$  quark matter (solid curves,  $n_d/T^3$  - top,  $n_u/T^3$  - bottom) or for including electrons and requiring  $\beta$ -equilibrium (dashed curves,  $n_d/T^3$ ,  $n_u/T^3$ ,  $n_e/T^3$  from top to bottom). For  $T = 1.1 T_c$ .

require  $\frac{2}{3}n_u - \frac{1}{3}n_d = 0$ . The according dependence  $\mu_d(\mu_u)$  is depicted in Fig. 6 (left panel) by the long-dashed curve, again for  $T = 1.1 T_c$ . More relevant for hypothetical very hot neutron star matter in a deconfined state is  $\beta$ -equilibrium. Flavor changing weak currents give rise to the balance equation  $d \leftrightarrow u + e + \bar{\nu}_e$ , i. e. in weak interaction equilibrium  $\mu_e = \mu_d - \mu_u$ , as the produced neutrinos are supposed to leave the star and do not participate in the balance. The electron net density is approximated by  $n_e = \frac{1}{3}\mu_e T^2 + \frac{1}{3\pi^2}\mu_e^3$ , and electrically neutral bulk matter is determined by  $\frac{2}{3}n_u - \frac{1}{3}n_d - n_e = 0$ . The corresponding dependence  $\mu_d(\mu_u)$  is depicted by the dash-dotted curve in Fig. 6 (left panel) for  $T = 1.1 T_c$ . The  $d$  quark net number density decreases by requiring  $\beta$ -equilibrium, demanding also a non-zero electron density for electrically neutral bulk matter (see Fig. 6 right panel);  $n_u$  is not affected when including electrons and  $\beta$ -equilibrium. This is in contrast to findings for the cold color-flavor locked phase of QCD [46] for  $N_f = 2 + 1$  dynamical quarks, where no electrons are required.

The discussion can easily be extended to the physically relevant case of two light (up and

down) and one heavier (strange) quarks, considering again two independent quark chemical potentials for the light quarks,  $\mu_l = \mu_u = \mu_d$ , and for the strange quark,  $\mu_s$ . Recently, first-principle lattice QCD data for this case became available [38, 45]. A detailed comparison of the properly extended quasiparticle model with these lattice results and, in particular, a discussion of finite baryon density effects on the EoS relevant for the hydrodynamical description of the expansion stage of heavy-ion collisions demands further studies.

#### IV. SUMMARY AND DISCUSSION

The focus of the present paper is an analysis of isovector and various flavor (off-)diagonal susceptibilities for two-flavor QCD by comparing the extended quasiparticle model with lattice QCD data [6, 12, 13]. The model includes the same quark mass parameters  $m_i$  as used in these lattice simulations. (Basically, one could accomplish also a chiral extrapolation. However, the effective coupling  $G^2(T)$  may implicitly depend on these masses. This deserves separate investigations.) A crucial point to be kept in mind concerns finite size effects. The lattice QCD calculations [6, 12, 13] are performed on grids with finite temporal and spatial extension, while our phenomenological model is formulated in the thermodynamic continuum limit. The use of an improved action in [12] lets us hope that the finite size effects are sufficiently small to make a direct comparison meaningful. In contrast, the lattice QCD data of [6, 13] require severe continuum extrapolation factors. In so far, the comparison of our extended QPM with these data is less direct.

Having these limitations in mind, we emphasize the good agreement of our model with the lattice QCD data for  $c_{2,4}$ ,  $c_{2,4}^I$ ,  $c_{2,4}^{uu}$  and  $c_4^{ud}$  as well as for the related generalized quark number susceptibilities. We consider this successful comparison as encouraging. A conclusion is that quasiparticle excitations, with a mass gap also in the chiral limit, are able to explain those features of the strongly coupled quark-gluon medium which are encoded in the mentioned coefficients. In particular, baryon density effects are probed by these coefficients. The baryon charge is carried by quasi-quark excitations, in contrast to models [19], where di-quark and three-quark modes carry a substantial fraction of the baryon charge. Furthermore, in several physical situations, like relativistic heavy-ion collisions or in hot proto-(quark) neutron stars, the various mentioned coefficients are needed to implement the adequate side conditions.

We have applied our model also for  $T < T_c$ . Formally, the description of the lattice QCD

data below  $T_c$  requires fairly large values of the effective coupling  $G^2(T)$ . (An alternative description could rely on strongly increasing correlations which are beyond the presently employed approach [47].) The corresponding excitations become very massive, ranging to hadronic mass scales. It turns out that a few massive excitations reproduce fairly well some of the lattice QCD data within the interval  $0.8 T_c - T_c$ . This is numerically not too distinct from the hadron resonance gas model, where one may regroup several resonances into a few representative effective excitations. (Vice versa, we mention that the resonance gas model [11, 12, 48] coincides with lattice QCD data also slightly above  $T_c$ ; for an even more extreme point of view we refer the interested reader to [49].) In this respect, it is conceivable that several models with fairly distinct assumptions may equally well reproduce the same lattice QCD data on thermodynamic bulk properties - examples are [19, 22–27, 50–52]. Only correlators and spectral properties of the excitations can unveil their real nature in the strongly interacting system.

On the other hand, the coefficient  $c_2^{ud}$ , and accordingly  $\chi_{1,1}$ , is poorly described. This may be a hint for missing modes or degrees of freedom in our model. Qualitatively, our findings can be understood since flavor-mixing effects, which are important for the correct description of the flavor off-diagonal susceptibility, are not explicitly inherent in our quasiparticle model, but only implicitly via the quasiparticle dispersion relations. Progressing lattice QCD calculations are welcome to resolve this issue and to get more confidence in the baryon number carrying modes (cf. discussions in [9, 18]). Also, the slight deviations between our model and the data very close to  $T_c$  may signal a deficit of our quasiparticle picture. Nevertheless, considering our phenomenological model as useful parametrization of lattice QCD results, it may serve as QCD-based input for hydrodynamical calculations for the expansion dynamics of matter created in ultra-relativistic heavy-ion collisions, cf. [34].

Finally, we stress that the utilized Taylor expansion technique is sensitive to the region  $\mu_{u,d} \rightarrow 0$ . QCD critical point effects at larger values of  $\mu_{u,d}$  may not be caught in such an approach. For a phenomenological procedure to supplement our model by critical point features see [53].

In summary, we extend our quasiparticle model towards two independent chemical potentials. This allows for the determination of various susceptibilities. We find an impressive agreement (with the exception of two numerically small flavor off-diagonal susceptibility coefficients) with lattice QCD data. Since a special set of susceptibilities also provides

the Taylor expansion coefficients of the baryon-driven excess pressure, we argue that our phenomenological quasiparticle model catches relevant modes for the equation of state at non-zero net baryon density. It may be used, therefore, for the future determination of higher-order Taylor expansion coefficients which become increasingly important at larger net baryon densities.

## Acknowledgements

We gratefully acknowledge discussions with E. Laermann, F. Karsch, R. V. Gavai and S. Gupta. The work is supported by BMBF 06DR136, GSI-FE, EU I3HP.

## Appendix A

The pressure  $p(T, \mu_u, \mu_d)$  as primary thermodynamic potential of our model is constructed by assuming a quasiparticle picture via

$$p(T, \mu_u, \mu_d) = \sum_{l=u,d,g} p_l(T, \mu_u, \mu_d) - B(\Pi_{u,d,g}[T, \mu_u, \mu_d]), \quad (37)$$

where  $B$  is to be determined as line integral from thermodynamic consistency conditions and the stationarity condition  $\delta p / \delta \Pi_j = 0$  resulting in  $\partial p_j / \partial \Pi_j = \partial B / \partial \Pi_j$ . The partial pressures  $p_l$  of included excitations  $l$  referring to  $u$  quarks,  $d$  quarks and gluons ( $g$ ) read

$$p_l = \epsilon_l d_l T \int \frac{d^3 k}{(2\pi)^3} \left[ \ln \left( 1 + \epsilon_l e^{-(\omega_l - \mu_l)/T} \right) + \ln \left( 1 + \epsilon_l e^{-(\omega_l + \mu_l)/T} \right) \right], \quad (38)$$

where the dispersion relations  $\omega_l = \omega_l(T, \mu_u, \mu_d)$  are given in Eqs. (4) and (5),  $\epsilon_l$  is  $+1$  ( $-1$ ) for fermions (bosons),  $d_l$  refers to the spin (polarization) and color degeneracies of quasiquarks and quasigluons reading  $d_u = d_d = 2 N_c$  and  $d_g = N_c^2 - 1$ , and  $\mu_g = 0$ . In this way, we count left-handed transversal quasigluons as anti-particles of the right-handed ones. These structures emerge from the underlying two-loop QCD  $\Phi$  functional [54, 55] by imposing formal manipulations such as neglecting finite width effects in the considered asymptotic HTL approximations of the one-loop self-energies, and neglecting (anti)plasmino and longitudinal gluon excitations as well as Landau damping [47]. While  $p$  is highly non-perturbative with respect to the effective coupling  $G^2$  entering the self-energy expressions, it is this phenomenologically introduced coupling which enables the model to go beyond the  $\Phi$ -derivable approximations in [55].

The entropy density expression entering the generalized Peshier equations in Eqs. (6-8) reads  $s = \sum_{l=u,d,g} s_l = \partial p / \partial T$  with

$$s_i = d_i \int \frac{d^3 k}{(2\pi)^3} \left[ \ln(1 + e^{-(\omega_i - \mu_i)/T}) + \frac{(\omega_i - \mu_i)/T}{(e^{(\omega_i - \mu_i)/T} + 1)} + (\mu_i \rightarrow -\mu_i) \right], \quad (39)$$

$$s_g = -2d_g \int \frac{d^3 k}{(2\pi)^3} \left[ \ln(1 - e^{-\omega_g/T}) - \frac{\omega_g/T}{(e^{\omega_g/T} - 1)} \right], \quad (40)$$

where  $i = u, d$  and  $\mu_u = \mu_q + \mu_I$ ,  $\mu_d = \mu_q - \mu_I$ . This additivity in the contributions  $s_l$  of the various parton species is anchored in the underlying two-loop QCD  $\Phi$  functional [47, 55, 56].

## Appendix B

The coefficients entering Eqs. (9 - 11) read

$$A_1 = \mathcal{I}_3 \frac{1}{3} \left[ 2T^2 + \frac{3}{2\pi^2} (\mu_q^2 + \mu_I^2) \right] + \mathcal{I}_4 \frac{1}{3} \left[ T^2 + \frac{1}{\pi^2} (\mu_q + \mu_I)^2 \right] + \mathcal{I}_5 \frac{1}{3} \left[ T^2 + \frac{1}{\pi^2} (\mu_q - \mu_I)^2 \right], \quad (41)$$

$$B_1 = -\mathcal{I}_1 \frac{1}{3} \left[ T^2 + \frac{1}{\pi^2} (\mu_q + \mu_I)^2 \right] + \mathcal{I}_2 \frac{1}{3} \left[ T^2 + \frac{1}{\pi^2} (\mu_q - \mu_I)^2 \right], \quad (42)$$

$$C_1 = -\mathcal{I}_3 \frac{1}{\pi^2} G^2 \mu_I - \mathcal{I}_4 \frac{1}{3} \frac{2}{\pi^2} [\mu_q + \mu_I] G^2 + \mathcal{I}_5 \frac{1}{3} \frac{2}{\pi^2} [\mu_q - \mu_I] G^2 + \mathcal{I}_1 \left( 2\xi_u^2 T + \frac{2}{3} T G^2 \right) - \mathcal{I}_2 \left( 2\xi_d^2 T + \frac{2}{3} T G^2 \right), \quad (43)$$

$$A_2 = \mathcal{I}_3 \frac{1}{3} \left[ 2T^2 + \frac{3}{2\pi^2} (\mu_q^2 + \mu_I^2) \right] + \mathcal{I}_4 \frac{1}{3} \left[ T^2 + \frac{1}{\pi^2} (\mu_q + \mu_I)^2 \right] + \mathcal{I}_5 \frac{1}{3} \left[ T^2 + \frac{1}{\pi^2} (\mu_q - \mu_I)^2 \right], \quad (44)$$

$$B_2 = -\mathcal{I}_1 \frac{1}{3} \left[ T^2 + \frac{1}{\pi^2} (\mu_q + \mu_I)^2 \right] - \mathcal{I}_2 \frac{1}{3} \left[ T^2 + \frac{1}{\pi^2} (\mu_q - \mu_I)^2 \right], \quad (45)$$

$$C_2 = -\mathcal{I}_3 \frac{1}{\pi^2} G^2 \mu_q - \mathcal{I}_4 \frac{1}{3} \frac{2}{\pi^2} [\mu_q + \mu_I] G^2 - \mathcal{I}_5 \frac{1}{3} \frac{2}{\pi^2} [\mu_q - \mu_I] G^2 + \mathcal{I}_1 \left( 2\xi_u^2 T + \frac{2}{3} T G^2 \right) + \mathcal{I}_2 \left( 2\xi_d^2 T + \frac{2}{3} T G^2 \right), \quad (46)$$

$$A_3 = \mathcal{I}_1 \frac{1}{3} \left[ T^2 + \frac{1}{\pi^2} (\mu_q + \mu_I)^2 \right], \quad (47)$$

$$B_3 = \mathcal{I}_2 \frac{1}{3} \left[ T^2 + \frac{1}{\pi^2} (\mu_q - \mu_I)^2 \right], \quad (48)$$

where the phase-space integrals  $\mathcal{I}_k$  are given by

$$\mathcal{I}_1 = \frac{\partial n_u}{\partial \Pi_u} = \frac{d_u}{2\pi^2} \int_0^\infty dk \frac{k^2}{2\omega_u T} \left( \frac{e^{(\omega_u + \mu_q + \mu_I)/T}}{(e^{(\omega_u + \mu_q + \mu_I)/T} + 1)^2} - \frac{e^{(\omega_u - \mu_q - \mu_I)/T}}{(e^{(\omega_u - \mu_q - \mu_I)/T} + 1)^2} \right), \quad (49)$$

$$\mathcal{I}_2 = \frac{\partial n_d}{\partial \Pi_d} = \frac{d_d}{2\pi^2} \int_0^\infty dk \frac{k^2}{2\omega_d T} \left( \frac{e^{(\omega_d + \mu_q - \mu_I)/T}}{(e^{(\omega_d + \mu_q - \mu_I)/T} + 1)^2} - \frac{e^{(\omega_d - \mu_q + \mu_I)/T}}{(e^{(\omega_d - \mu_q + \mu_I)/T} + 1)^2} \right), \quad (50)$$

$$\mathcal{I}_3 = \frac{\partial s_g}{\partial \Pi_g} = -\frac{d_g}{\pi^2} \int_0^\infty dk \frac{k^2}{2T^2} \frac{e^{\omega_g/T}}{(e^{\omega_g/T} - 1)^2}, \quad (51)$$

$$\mathcal{I}_4 = \frac{\partial s_u}{\partial \Pi_u} = -\frac{d_u}{2\pi^2} \int_0^\infty dk \frac{k^2}{2\omega_u T^2} \left( \frac{(\omega_u + \mu_q + \mu_I)e^{(\omega_u + \mu_q + \mu_I)/T}}{(e^{(\omega_u + \mu_q + \mu_I)/T} + 1)^2} + (\mu_{q,I} \rightarrow -\mu_{q,I}) \right), \quad (52)$$

$$\mathcal{I}_5 = \frac{\partial s_d}{\partial \Pi_d} = -\frac{d_d}{2\pi^2} \int_0^\infty dk \frac{k^2}{2\omega_d T^2} \left( \frac{(\omega_d + \mu_q - \mu_I)e^{(\omega_d + \mu_q - \mu_I)/T}}{(e^{(\omega_d + \mu_q - \mu_I)/T} + 1)^2} + (\mu_{q,I} \rightarrow -\mu_{q,I}) \right). \quad (53)$$

In Eqs. (14) and (15),  $\mu_q$  and  $\mu_I$  in the phase-space integrals  $\mathcal{I}_k$  are replaced by  $\mu_u = \mu_q + \mu_I$  and  $\mu_d = \mu_q - \mu_I$ .

## Appendix C

The coefficients in Eqs. (12) and (13) read

$$\mathcal{A}_1 = \mathcal{A}_2 = \frac{1}{3}\mathcal{I}_3 \left[ 2T^2 + \frac{3}{4\pi^2} (\mu_u^2 + \mu_d^2) \right] + \frac{1}{3}\mathcal{I}_4 \left[ T^2 + \frac{\mu_u^2}{\pi^2} \right] + \frac{1}{3}\mathcal{I}_5 \left[ T^2 + \frac{\mu_d^2}{\pi^2} \right], \quad (54)$$

$$\mathcal{B}_1 = \mathcal{B}_2 = -\frac{1}{3}\mathcal{I}_1 \left[ T^2 + \frac{\mu_u^2}{\pi^2} \right] \quad (55)$$

and

$$\mathcal{C}_1 = \mathcal{I}_1 \left( 2\xi_u^2 T + \frac{2}{3} T G^2 \right) - \mathcal{I}_3 \frac{1}{2\pi^2} G^2 \mu_u - \mathcal{I}_4 \frac{2}{3\pi^2} \mu_u G^2, \quad (56)$$

$$\begin{aligned} \mathcal{C}_2 = & \mathcal{I}_1 \frac{(T^2 + \mu_u^2/\pi^2)}{(T^2 + \mu_d^2/\pi^2)} \left( 2\xi_d^2 T + \frac{2}{3} T G^2 \right) - \mathcal{I}_3 \frac{1}{2\pi^2} G^2 \mu_d \frac{\mathcal{I}_1}{\mathcal{I}_2} \frac{(T^2 + \mu_u^2/\pi^2)}{(T^2 + \mu_d^2/\pi^2)} \\ & - \mathcal{I}_5 \frac{2}{3\pi^2} \mu_d G^2 \frac{\mathcal{I}_1}{\mathcal{I}_2} \frac{(T^2 + \mu_u^2/\pi^2)}{(T^2 + \mu_d^2/\pi^2)}, \end{aligned} \quad (57)$$

where  $\mu_q$  and  $\mu_I$  in the phase-space integrals  $\mathcal{I}_k$  defined in Appendix B have to be substituted by  $\mu_u = \mu_q + \mu_I$  and  $\mu_d = \mu_q - \mu_I$ . The coefficients in Eq. (16) read

$$\mathcal{N} = T^2 \left( \frac{2}{3}\mathcal{I}_3 + \frac{1}{3}\mathcal{I}_4 + \frac{1}{3}\mathcal{I}_5 \right), \quad (58)$$

$$\mathcal{N}_1 = \frac{d_u}{2\pi^2} \int_0^\infty dk \frac{k^2}{T^2 \omega_u} \left( \frac{e^{\omega_u/T}}{(e^{\omega_u/T} + 1)^2} - 2 \frac{e^{2\omega_u/T}}{(e^{\omega_u/T} + 1)^3} \right), \quad (59)$$

$$\mathcal{N}_2 = \frac{d_d}{2\pi^2} \int_0^\infty dk \frac{k^2}{T^2 \omega_d} \left( \frac{e^{\omega_d/T}}{(e^{\omega_d/T} + 1)^2} - 2 \frac{e^{2\omega_d/T}}{(e^{\omega_d/T} + 1)^3} \right), \quad (60)$$

where  $\mathcal{I}_{3,4,5}$  as well as  $\omega_{u,d}$  have to be taken at  $\mu_q = \mu_I = 0$  or, equivalently,  $\mu_u = \mu_d = 0$ .

## Appendix D

Let us first briefly discuss an implication of the requirement  $\mu_{u,d} \ll \pi T$  needed for the consistency of Eqs. (12) and (13). Second-order susceptibility coefficients depend on  $G^2$  evaluated at  $\mu_{u,d} = 0$ , while fourth-order coefficients depend on  $G^2$  and  $\partial^2 G^2 / \partial \mu_{u,d}^2$  at  $\mu_{u,d} = 0$ . In general,  $n$ -th order derivatives of  $G^2$  require up to and including  $(n - 1)$ -st derivatives of  $\mathcal{C}_1$  or  $\mathcal{C}_2$ . This implies that up to and including third-order the derivatives of the effective coupling can trustfully be taken. Therefore, second- and fourth-order susceptibility coefficients and related quantities are uniquely determined. However,  $\left. \frac{\partial^4 G^2}{\partial \mu_u^4} \right|_{\mu_u = \mu_d = 0}$  and higher orders cannot be evaluated uniquely. These derivatives enter, for instance, sixth- and higher-order susceptibility coefficients.

The origin of this insanity is the special ansatz for the self-energy parts in the quasiparticle dispersion relations in Eqs. (4) and (5), while our primary thermodynamic potential in Eq. (37) together with (38) should allow for consistency in all orders of powers of  $\mu_{u,d}$ . The reasoning for our ansatz in Eqs. (4) and (5) is the contact to one-loop expressions for the self-energies [57]. It has been shown, however, in [58], for one (imaginary) chemical potential, that one can discard the explicit  $\mu^2$  terms in the self-energies and obtains an equally suitable description of the lattice QCD results. In other words, the stationarity property of the thermodynamic potential  $p$ , involved in our quasiparticle model, causes a robustness against such modifications of the employed self-energy parametrizations.

It happens that for the modified self-energies,  $\Pi_i = \frac{1}{3}T^2 G^2(T, \mu_u, \mu_d)$  and  $\Pi_g = \frac{2}{3}T^2 G^2(T, \mu_u, \mu_d)$ , the coefficients in Eqs. (12) and (13) render to

$$\mathcal{A}_1 = \mathcal{A}_2 = \frac{T^2}{3} (2\mathcal{I}_3 + \mathcal{I}_4 + \mathcal{I}_5) , \quad (61)$$

$$\mathcal{B}_1 = \mathcal{B}_2 = -\frac{T^2}{3} \mathcal{I}_1 , \quad (62)$$

$$\mathcal{C}_1 = \mathcal{C}_2 = \frac{2}{3} T G^2 \mathcal{I}_1 , \quad (63)$$

(for simplicity, we consider here the chiral limit or, as in section IIIB, temperature independent bare quark masses). I. e. the generalized system of flow equations in Eqs. (9-11) is uniquely solvable without restrictions, and  $G^2$  and all its derivatives are trustfully obtained, implying also a consistent determination of the susceptibility coefficients of arbitrary order opening the avenue for future investigations. We have checked numerically that the result exhibited for the fourth-order coefficient in Fig. 4 is changed by less than 9% when changing

the self-energy expressions (generically a slight down shift of the curves occurs). The result for the second-order coefficient exhibited in Fig. 4 remains unchanged as it depends only on  $G^2$  at  $\mu_{u,d} = 0$  which is not affected by the modification of the self-energy parametrizations. Similar statements are applicable for other related susceptibilities. Consequently, the results exhibited in Figs. 5 and 6 remain effectively unaltered.

- 
- [1] E. V. Shuryak, Prog. Part. Nucl. Phys. **53**, 273 (2004); Nucl. Phys. A **750**, 64 (2005).
  - [2] M. Gyulassy, and L. McLerran, Nucl. Phys. A **750**, 30 (2005).
  - [3] D. A. Teaney, Phys. Rev. C **68**, 034913 (2003); J. Phys. G **30**, S1247 (2004); Nucl. Phys. A **785**, 44 (2007).
  - [4] Proceedings of Critical Point and Onset of Deconfinement - 3rd International Workshop, July 3-6, 2006, Florence, Italy, (Ed.) F. Becattini; 4th International Workshop, July 9-13, 2007, Darmstadt, Germany, (Eds.) P. Senger et al.
  - [5] Z. Fodor, and S. Katz, J. High Energy Phys. **0203**, 014 (2002); J. High Energy Phys. **0404**, 050 (2004).
  - [6] R. V. Gavai, and S. Gupta, Phys. Rev. D **71**, 114014 (2005).
  - [7] C. R. Allton, S. Ejiri, S. J. Hands, O. Kaczmarek, F. Karsch, E. Laermann, C. Schmidt, and L. Scorzato, Phys. Rev. D **66**, 074507 (2002).
  - [8] V. Koch, A. Majumder, and J. Randrup, Phys. Rev. Lett. **95**, 182301 (2005).
  - [9] R. V. Gavai, and S. Gupta, Phys. Rev. D **73**, 014004 (2006).
  - [10] R. V. Gavai, S. Gupta, and P. Majumdar, Phys. Rev. D **65**, 054506 (2002).
  - [11] C. R. Allton, S. Ejiri, S. J. Hands, O. Kaczmarek, F. Karsch, E. Laermann, and C. Schmidt, Phys. Rev. D **68**, 014507 (2003).
  - [12] C. R. Allton, M. Döring, S. Ejiri, S. J. Hands, O. Kaczmarek, F. Karsch, E. Laermann, and K. Redlich, Phys. Rev. D **71**, 054508 (2005).
  - [13] R. V. Gavai, and S. Gupta, Phys. Rev. D **72**, 054006 (2005).
  - [14] Y. Maezawa, T. Hatsuda, S. Aoki, K. Kanaya, S. Ejiri, N. Ishii, N. Ukita, and T. Umeda, PoS **LAT2007**, 207 (2007).
  - [15] A. Hietanen, and K. Rummukainen, PoS **LAT2006**, 137 (2006).
  - [16] C. Bernard, T. Burch, C. E. DeTar, J. Osborn, S. Gottlieb, E. B. Gregory, D. Toussaint,



- U. M. Heller, and R. Sugar, Phys. Rev. D **71**, 034504 (2005); C. Bernard, T. Burch, C. E. DeTar, S. Gottlieb, L. Levkova, U. M. Heller, J. E. Hetrick, D. B. Renner, D. Toussaint, and R. Sugar, PoS **LAT2006**, 139 (2006); C. Bernard, T. Burch, C. E. DeTar, L. Levkova, S. Gottlieb, U. M. Heller, J. E. Hetrick, R. Sugar, and D. Toussaint, PoS **LAT2007**, 190 (2007); C. Bernard, C. E. DeTar, L. Levkova, S. Gottlieb, U. M. Heller, J. E. Hetrick, R. Sugar, and D. Toussaint, Phys. Rev. D **77**, 014503 (2008).
- [17] S. Mukherjee, Phys. Rev. D **74**, 054508 (2006).
- [18] F. Karsch, S. Ejiri, and K. Redlich, Nucl. Phys. A **774**, 619 (2006); S. Ejiri, F. Karsch, and K. Redlich, Phys. Lett. B **633**, 275 (2006).
- [19] J. Liao, and E. V. Shuryak, Phys. Rev. D **73**, 014509 (2006).
- [20] E. V. Shuryak, and I. Zahed, Phys. Rev. D **70**, 054507 (2004); B. A. Gelman, E. V. Shuryak, and I. Zahed, Phys. Rev. C **74**, 044908 (2006).
- [21] A. Peshier, and W. Cassing, Phys. Rev. Lett. **94**, 172301 (2005); W. Cassing, Nucl. Phys. A **795**, 70 (2007).
- [22] C. Sasaki, B. Friman, and K. Redlich, Phys. Rev. D **75**, 054026 (2007).
- [23] C. Sasaki, B. Friman, and K. Redlich, Phys. Rev. D **75**, 074013 (2007).
- [24] S. K. Ghosh, T. K. Mukherjee, M. G. Mustafa, and R. Ray, Phys. Rev. D **73**, 114007 (2006); arXiv:0710.2790 [hep-ph].
- [25] S. Rößner, C. Ratti, and W. Weise, Phys. Rev. D **75**, 034007 (2007); Phys. Lett. B **649**, 57 (2007).
- [26] V. M. Bannur, Eur. Phys. J. C **50**, 629 (2007).
- [27] B. Kämpfer, M. Bluhm, H. Schade, R. Schulze, and D. Seipt, PoS **CPOD2007**, 007 (2007).
- [28] J.-P. Blaizot, I. Iancu, and A. Rebhan, Phys. Lett. B **523**, 143 (2001).
- [29] G. Boyd, S. Gupta, and F. Karsch, Nucl. Phys. B **385**, 481 (1992); P. Petreczky, F. Karsch, E. Laermann, S. Stickan, and I. Wetzorke, Nucl. Phys. Proc. Suppl. **106**, 513 (2002).
- [30] F. Karsch, and M. Kitazawa, Phys. Lett. B **658**, 45 (2007).
- [31] A. Peshier, B. Kämpfer, O. P. Pavlenko, and G. Soff, Phys. Lett. B **337**, 235 (1994); Phys. Rev. D **54**, 2399 (1996).
- [32] A. Peshier, B. Kämpfer, and G. Soff, Phys. Rev. C **61**, 045203 (2000); Phys. Rev. D **66**, 094003 (2002).
- [33] M. Bluhm, B. Kämpfer, and G. Soff, Phys. Lett. B **620**, 131 (2005).

- [34] M. Bluhm, B. Kämpfer, R. Schulze, D. Seipt, and U. Heinz, Phys. Rev. C **76**, 034901 (2007).
- [35] A. Peshier, private communication, 2002.
- [36] D. Seipt, Diploma Thesis, *Quark mass dependence of one-loop self-energies in hot QCD*, Technische Universität Dresden, Germany, May 2007.
- [37] Y. Hatta, and M. A. Stephanov, Phys. Rev. Lett. **91**, 102003 (2003).
- [38] F. Karsch, arXiv:0711.0656 [hep-lat].
- [39] F. Karsch, E. Laermann, and A. Peikert, Phys. Lett. B **478**, 447 (2000).
- [40] F. Karsch, private communication, January 2006.
- [41] R. V. Gavai, and S. Gupta, Phys. Rev. D **65**, 094515 (2002); Phys. Rev. D **67**, 034501 (2003); private communication, March 2006.
- [42] R. V. Gavai, and S. Gupta, Phys. Rev. D **68**, 034506 (2003).
- [43] A. Rebhan, and P. Romatschke, Phys. Rev. D **68**, 025022 (2003).
- [44] S. Mukherjee, M. G. Mustafa, and R. Ray, Phys. Rev. D **75**, 094015 (2007).
- [45] C. Miao, and C. Schmidt, PoS **LAT2007**, 175 (2007).
- [46] K. Rajagopal, and F. Wilczek, Phys. Rev. Lett. **86**, 3492 (2001).
- [47] M. Bluhm, B. Kämpfer, R. Schulze, and D. Seipt, Eur. Phys. J. C **49**, 205 (2007).
- [48] F. Karsch, K. Redlich, and A. Tawfik, Phys. Lett. B **571**, 67 (2003).
- [49] D. B. Blaschke, and K. A. Bugaev, Phys. Part. Nucl. Lett. **2**, 305 (2005).
- [50] M. Procura, B. U. Musch, T. Wollenweber, T. R. Hemmert, and W. Weise, Phys. Rev. D **73**, 114510 (2006).
- [51] A. S. Khvorostukin, V. V. Skokov, V. D. Toneev, and K. Redlich, Eur. Phys. J. C **48**, 531 (2006); Yu. B. Ivanov, A. S. Khvorostukhin, E. E. Kolomeitsev, V. V. Skokov, V. D. Toneev, and D. N. Voskresensky, Phys. Rev. C **72**, 025804 (2005).
- [52] T. S. Biro, P. Levai, P. Van, and J. Zimanyi, Phys. Rev. C **75**, 034910 (2007).
- [53] M. Bluhm, and B. Kämpfer, PoS **CPOD2006**, 004 (2006); B. Kämpfer, M. Bluhm, R. Schulze, D. Seipt, and U. Heinz, Nucl. Phys. A **774**, 757 (2006).
- [54] G. Baym, Phys. Rev. **127**, 1391 (1962).
- [55] J.-P. Blaizot, E. Iancu, and A. Rebhan, Phys. Rev. Lett. **83**, 2906 (1999); Phys. Lett. B **470**, 181 (1999); Phys. Rev. D **63**, 065003 (2001); Phys. Rev. D **68**, 025011 (2003); and in *Quark Gluon Plasma 3*, edited by R. C. Hwa and X. N. Wang (World Scientific, Singapore, 2004), p. 60.

- [56] B. Vanderheyden, and G. Baym, J. Stat. Phys. **93**, 843 (1998); and in *Progress in Nonequilibrium Green's functions*, (Ed.) M. Bonitz (World Scientific, Singapore, 2000).
- [57] M. Le Bellac, *Thermal Field Theory* (Cambridge University Press, Cambridge, 1996).
- [58] M. Bluhm, and B. Kämpfer, Phys. Rev. D **77**, 034004 (2008).